RESEARCH PAPERS

Acta Cryst. (1996). A**52**, 340–348

Planar Facet Interface: Overlapping Volume and Scherrer Constant Expressions

SALVINO CICCARIELLO[a]* AND ROGER SOBRY[b]

[a]*INFM-Dipartimento di Fisica 'G. Galilei', via Marzolo 8, I-35131 Padova, Italy, and* [b]*Laboratory of Experimental Physics, Institute of Physics B5, University of Liège, Sart Tilman, B-4000 Liège, Belgium. E-mail: ciccariello@padova.infn.it*

(*Received 22 June 1995; accepted 10 November 1995*)

Abstract

For powder samples made up of crystallites with planar facets, the domain where the overlapping volume function is defined can be split into intervals where the overlapping volume function turns out to be a cubic. A method of calculating the coefficients of each cubic function is illustrated. The coefficients of the cubic, relevant to the interval containing the origin, are related to Scherrer constants $\mathcal{K}_K$, $\mathcal{K}_T$ and to the rotundity parameter $\mathcal{M}$. Their expressions are worked out and numerically illustrated for dodecahedra, icosahedra and triclinic parallelepipeds. The general functional expression of peak profiles relevant to planar facets is also given.

1. Introduction

The peak profile [$\equiv I_{\mathbf{h}}(s)$] around a reflection $\mathbf{h} = (h, k, l)$ is fully determined by the only interphase surface when the crystallites, constituting the powder sample, have a negligible lattice disorder† (Wilson, 1962*a*; Guinier, 1963). In reality, this condition is rarely met and might explain why the interest in finding explicit relations between peak profiles and geometrical features of interfaces have considerably decreased since the early 60's, when most of the presently available results (Wilson, 1970) were obtained. Nonetheless, further theoretical results on this issue can be obtained under the rather mild assumption that a sample's crystallites have *planar* facets. This configuration was analyzed by Grebille & Bérar (1985) under the further assumption that crystallites have a *convex* polyhedrical shape. These authors‡ showed that each polyhedral crystallite can be decomposed into triangular truncated prisms and reported the peak profile expressions for the three possible shapes of the resulting triangular truncated prisms. These expressions depend on the lengths of the three edges parallel to the considered reflection direction. [See their equations (6), (8) and (9).] In this way, the general expression of peak profiles for samples consisting of equal *convex* polyhedra was obtained in terms of the lengths of the parallel edges resulting from this decomposition.

The aim of this paper is to make the analysis of this geometrical configuration more complete by using a general property of the corresponding overlapping volume function [$V_{\hat{\mathbf{h}}}(r)$], more simply referred to as the overlap function (OF). The OF yields the volume common to the filled parts of the sample and of the 'ghost' resulting from the translation of the sample by r along $\hat{\mathbf{h}}$, the direction of reflection $\mathbf{h}$. The general property of the OF that will be proven in this paper is: for samples made up of crystallites with planar facets, the overlap function $V_{\hat{\mathbf{h}}}(r)$ is

$$V_{\hat{\mathbf{h}}}(r) = \sum_{l=0}^{3} \Gamma_{l,i}(r - D_i)^l,$$

$$D_i < r < D_{i+1}, \quad i = 0, 1, \ldots, N-1. \qquad (1)$$

In other words, the interval $[0, R_{\max}]$, where $V_{\hat{\mathbf{h}}}(r)$ is defined, splits into the subintervals $[D_i, D_{i+1}]$, $i = 0, 1, \ldots, N-1$, with $D_0 = 0$ and $D_N = R_{\max}$, and in each of these $V_{\hat{\mathbf{h}}}(r)$ is a *cubic* function. Wilson (1962*a*) has already remarked that the OF is a cubic for rectangular parallelepipeds, tetrahedra and octahedra. According to (1), this property simply follows from the planarity of the facets. Moreover, (1) also implies that the inverse Fourier transforms of the peak profiles reported by Grebille & Bérar (1985) must have the analytic expression (1) because the profiles are relevant to particles with planar facets; this could be used to prove (1). However, the present analysis is based on the integral expression of the second-order derivative $V''_{\hat{\mathbf{h}}}(r)$ of the OF. This approach presents three advantages: (i) the convexity assumption can be removed; (ii) the explicit functional expression of $V_{\hat{\mathbf{h}}}(r)$ can be obtained in terms of geometrical parameters more directly related to the interface geometry, *i.e.* the dihedral angles, the angles between the edges entering each vertex and the

† Of course, it is assumed that the corrections related to background scattering, wavelength dispersion, finite size of the collimation slits and other geometrical factors have been taken into account.

‡ We are grateful to the referee who brought this paper to our attention.

lengths of the edges; (iii) the expressions of Scherrer constants $\mathcal{K}_K$, $\mathcal{K}_T$ as well as that of $\mathcal{M}$, the *rotundity* parameter (see *e.g.* Langford & Wilson, 1978), are also obtained; they are simply related to coefficients $\Gamma_{1,0}$, $\Gamma_{2,0}$ and $\Gamma_{3,0}$, whose explicit expressions will be evaluated later.

The paper is organized as follows. §2 reports some general definitions required by the analysis to be carried out in the following sections. Result (1) is worked out in §3. The explicit expressions for $\mathcal{K}_K$, $\mathcal{K}_T$ and $\mathcal{M}$ as well as a numerical application of these formulae to the cases of dodecahedra, icosahedra and triclinic parallelepipeds are reported in §4. Finally, the implications of (1) in determining the analytic form of peak profiles are discussed in §5.

2. Basic formulae

The overlap function $V_{\hat{\mathbf{h}}}(r)$ is related to the so-called oriented stick probability function (OSPF) $\gamma_{\mathbf{h}}(r)$, defined as (Ciccariello, 1985)

$$\gamma_{\mathbf{h}}(r) = V_F^{-1} \int_{R^3} \mathrm{d}v_1 \, \rho_F(\mathbf{r}_1 + r\mathbf{h})\rho_F(\mathbf{r}_1), \qquad (2a)$$

by the simple relation

$$V_{\hat{\mathbf{h}}}(r) = V_F \gamma_{\mathbf{h}}(r/|\mathbf{h}|) \qquad (2b)$$

(see Ciccariello, 1990, §§II and III). Here, V_F denotes the total volume of the only crystallites of the sample (*i.e.* V_F is the volume of the filled part of the sample) while function $\rho_F(\mathbf{r})$ is defined as being equal to 1 when the tip of $\mathbf{r}$ falls inside the filled part of the sample and equal to 0 elsewhere. The definition of $\gamma_{\mathbf{h}}(r)$ generalizes that of the correlation function introduced by Debye, Anderson & Brumberger (1957) in the realm of small-angle X-ray scattering (SAXS). Indeed, since definition (2*a*) makes sense even when $\mathbf{h}$ is not a point of the reciprocal lattice, the SAXS correlation function is the angular average, with respect to all possible orientations of $\mathbf{h}$, of the OSPFs $\gamma_{\mathbf{h}}(r)$. Since the latter is proportional to the OF at the lattice points, it appears evident that small- and wide-angle scattering are strongly related (Ciccariello, 1990).

Equation (2*a*), in terms of Dirac's function, reads

$$\gamma_{\mathbf{h}}(r) = V_F^{-1} \int_{V_F} \mathrm{d}v_1 \int_{V_F} \mathrm{d}v_2 \, \delta(\mathbf{r}_1 + r\mathbf{h} - \mathbf{r}_2). \qquad (3)$$

Equations (2) and (3) show that $\gamma_{\mathbf{h}}(r)$ only depends on the geometry of crystallite boundaries and on the latter disposition in the space, when these are observed along direction $\hat{\mathbf{h}} \equiv \mathbf{h}/|\mathbf{h}|$. They also imply that

$$\gamma_{p\mathbf{h}}(r/p) = \gamma_{\mathbf{h}}(r), \qquad p \in Z^+, \qquad (4a)$$

$$\gamma_{\mathbf{h}}(r) = \gamma_{\mathbf{h}}(-r). \qquad (4b)$$

These properties will be referred to as the scaling and the parity properties. Moreover, (3) ensures that $\gamma_{\mathbf{h}}(r)$ is such that, at any point r, $\gamma_{\mathbf{h}}(r^-) = \gamma_{\mathbf{h}}(r^+)$. Then, with the assumption that (1) has already been proved, from (2*b*) at $r = D_i$, $V_{\hat{\mathbf{h}}}(D_i^-) = V_{\hat{\mathbf{h}}}(D_i^+)$. Hence,

$$\sum_{l=0}^{3} \Gamma_{l,i-1}(D_i - D_{i-1})^l = \Gamma_{0,i}, \quad i = 1, 2, \ldots, N-1. \qquad (5)$$

Owing to the property $\gamma_{\mathbf{h}}(0) = 1$, from (2*b*) and (1) at $r = D_0 = 0$, it follows that $\Gamma_{0,0} = V_F$. Then, (5) can be used in order to determine recursively all the remaining $\Gamma_{0,i}$'s with $i > 0$. It turns out that each $\Gamma_{0,i}$, with $i > 0$, depends on the $\Gamma_{l,j}$'s with $1 \le l \le 3$ and $0 \le j \le i-1$, as well as V_F $(= \Gamma_{0,0})$.

In order to prove (1) and to obtain a method of calculating the $\Gamma_{m,i}$'s, it is convenient to recall the integral expressions of the first and second derivatives of OSPF worked out by Ciccariello (1985):

$$\gamma'_{\mathbf{h}}(r) = \int_{\mathcal{S}_F} \mathrm{d}S_1 \, (\mathbf{h} \cdot \hat{\boldsymbol{\sigma}}_1)\rho_F(\mathbf{r}_1 + r\mathbf{h})/V_F, \qquad (6)$$

$$\gamma''_{\mathbf{h}}(r) = -\int_{\mathcal{S}_F} \mathrm{d}S_1 \, (\mathbf{h} \cdot \hat{\boldsymbol{\sigma}}_1) \times \int_{\mathcal{S}_F} \mathrm{d}S_2 \, (\mathbf{h} \cdot \hat{\boldsymbol{\sigma}}_2)\delta(\mathbf{r}_1 + r\mathbf{h} - \mathbf{r}_2)/V_F. \qquad (7)$$

Here, $\mathcal{S}_F$ denotes the interface, *i.e.* the surface bounding the filled part of the sample, and $\hat{\boldsymbol{\sigma}}_i$ $(i = 1, 2)$ denotes the unit vector orthogonal to $\mathrm{d}S_i$ and pointing outwardly to the filled region.

3. The local cubic structure

The proof that the OF behaves in each interval as a cubic function can be obtained from (7) by exploiting the property that the interface consists of $\mathcal{N}$ planar facets. The analysis closely follows a recent paper by Ciccariello & Sobry (1995), devoted to some SAXS aspects of the problem and referred to as paper I in the following. Let $\mathcal{F}_i$ denote the ith planar facet of interface $\mathcal{S}_F$ so that $\mathcal{S}_F = \cup_{i=1}^{\mathcal{N}} \mathcal{F}_i$. Then, by (2*b*) and (7), the second derivative of $V_{\hat{\mathbf{h}}}(r)$ splits into a sum of integrals, *i.e.*

$$V''_{\hat{\mathbf{h}}}(r) = \sum_{i,j=1}^{\mathcal{N}} \mathcal{P}^{(2)}_{i,j}(r), \qquad (8)$$

where

$$\mathcal{P}^{(2)}_{i,j}(r) \equiv -\int_{\mathcal{F}_i} \mathrm{d}S_1 \, (\hat{\mathbf{h}} \cdot \hat{\boldsymbol{\sigma}}_i) \times \int_{\mathcal{F}_j} (\hat{\mathbf{h}} \cdot \hat{\boldsymbol{\sigma}}_j) \, \mathrm{d}S_2 \, \delta(\mathbf{r}_1 + r\hat{\mathbf{h}} - \mathbf{r}_2) \qquad (9)$$

is the contribution to the second derivative owing to the facet pair (i, j). [The dependence on $\hat{\mathbf{h}}$ is not reported on

the left side of (9) for notational simplicity.] From (9), it is evident that $\mathcal{P}^{(2)}_{i,j}(r) = \mathcal{P}^{(2)}_{j,i}(r)$ and $\mathcal{P}^{(2)}_{i,i}(r) = 0$. (The latter follows from the fact the integrand is null because Dirac's function requires that $r\hat{\mathbf{h}} = \mathbf{r}_1 - \mathbf{r}_2$ and, since $\mathbf{r}_1$ and $\mathbf{r}_2$ are points of $\mathcal{F}_i$, $r\hat{\mathbf{h}}$ turns out to be orthogonal to $\hat{\boldsymbol{\sigma}}_i$.) Then, (8) becomes

$$V''_{\hat{\mathbf{h}}}(r) = 2 \sum_{1 \le i < j \le \mathcal{N}} \mathcal{P}^{(2)}_{i,j}(r). \qquad (10a)$$

The proof of (1) is trivial once it has been shown that the range of r's, where each $\mathcal{P}^{(2)}_{i,j}(r)$ is defined, splits into subintervals $[D_{ij,k}, D_{ij,k+1}]$, with $D_{ij,k} < D_{ij,k+1}$ and $k = 0, 1, \ldots, (N_{ij} - 1)$, and that in each of these $\mathcal{P}^{(2)}_{i,j}(r)$ turns out to be a *linear* r function. Indeed, assume that this result has already been proven. Then,

$$[0, R_{\max}] = [0, D_N] = \bigcup_{\substack{1 \le i < j \le \mathcal{N} \\ 0 \le k \le (N_{ij}-1)}} [D_{ij,k}, D_{ij,k+1}].$$

Consider now the finer decomposition resulting from the intersection operations

$$[D_{ij,k}, D_{ij,k+1}] \bigcap [D_{i'j',k'}, D_{i'j',k'+1}]$$

for all possible values of the involved indices. By so doing, the interval $[0, R_{\max}]$ will be split into the subintervals $[D_i, D_{i+1}]$ (with $D_i < D_{i+1}$, $D_0 = 0$ and $i = 0, 1, \ldots, N - 1$) such that in each of these each $\mathcal{P}^{(2)}_{i,j}(r)$ has a well defined linear expression (eventually equal to zero). Consequently, the (linear) expression of $V''_{\hat{\mathbf{h}}}(r)$ turns out to be determined in each subinterval $[D_i, D_{i+1}]$ by (10*a*). Then, two subsequent quadratures yield

$$V_{\hat{\mathbf{h}}}(r) = \int_r^{R_{\max}} (r - t) V''_{\hat{\mathbf{h}}}(t)\, \mathrm{d}t \qquad (10b)$$

and the explicit *cubic* expression (1) of $V_{\hat{\mathbf{h}}}(r)$ is obtained in the subinterval $[D_i, D_{i+1}]$ in which the considered r value lies. Thus, the proof of (1) will be accomplished once the linear r dependence of each $\mathcal{P}^{(2)}_{i,j}(r)$ and the associated subintervals have been determined.

To achieve this goal, consider a pair of facets, say $\mathcal{F}_i$ and $\mathcal{F}_j$ with $i \neq j$, lying on planes Π_i and Π_j. These can be coinciding, parallel or intersecting. In the first case, $\mathcal{P}^{(2)}_{i,j}(r)$ is identically equal to zero for the same reason that $\mathcal{P}^{(2)}_{i,i}(r) = 0$. For the other cases, it is noted that (9) ensures that $\mathcal{P}^{(2)}_{i,j}(r)$ can differ from zero only when $\mathcal{F}_i$, translated by $r\hat{\mathbf{h}}$, intersects $\mathcal{F}_j$. [This condition is required by the Dirac function present in the integrand of (9). For later convenience, it is also noted that, when $r = 0$, the same function will require that $\mathcal{F}_i$ touches $\mathcal{F}_j$ for $\mathcal{P}^{(2)}_{i,j}(r)$ to be different from zero. Then, clearly, if the contact takes place at a point, this will be a vertex of the interface while, if it takes place along a segment, this will be (part of) an edge.] Thus, in the second case, $\mathcal{P}^{(2)}_{i,j}(r)$ is equal to zero unless r is equal to the distance (evaluated along direction $\hat{\mathbf{h}}$) of Π_i from Π_j, a possibility that will be assumed not to take place in the following for reasons of simplicity.* The last case, that of intersecting Π_i and Π_j, is the most interesting one. In this case, Π_i and Π_j can be restricted to the half-planes containing facets $\mathcal{F}_i$ and $\mathcal{F}_j$. Fig. 1 depicts a typical configuration where facet $\mathcal{F}_i$, translated by $r\hat{\mathbf{h}}$, intersects facet $\mathcal{F}_j$. The superposing segments, shown in bold, lie respectively on lines a and b parallel to OO', the intersection line of the two half-planes. When r is slightly increased, lines a and b will move respectively towards the right and the left of the figure. Owing to the polygonal shape of the $\mathcal{F}_i$ and $\mathcal{F}_j$ boundaries, the length of the intersection segment will be a linear function of r, whose numerical coefficients depend on the sides of $\mathcal{F}_i$ and $\mathcal{F}_j$ that delimit the superposing segments. Further, the figure makes it evident that the sides do not change as r varies in an interval such that a moves inside one of the intervals $[A'_l, A'_m]$ and, simultaneously, b moves inside one of the $[B'_p, B'_q]$'s. {Point A'_l (B'_l) is the orthogonal projection of vertex A_l (B_l) of $\mathcal{F}_i$ ($\mathcal{F}_j$) on the axis X (Y). Moreover, the extrema of each interval, for instance $[A'_4, A'_2]$ or $[B'_1, B'_2]$, are nearest-neighbor points on X or on Y.} These properties and the fact that integral (9), for simple dimensional reasons, is proportional to the

* Indeed, whenever this happens, at this particular value, denoted by r_0, $\mathcal{P}^{(2)}_{i,j}(r)$ is proportional to $\delta(r - r_0)$ and the proportionality coefficient depends on the area of the overlapping surfaces between $\mathcal{F}_j$ and $\mathcal{F}_i$, translated by $r_0\hat{\mathbf{h}}$ (Ciccariello, 1985). Hence, these δ-like contributions are known and can be simply accounted for, though the final expression of the OF will be slightly more involved.

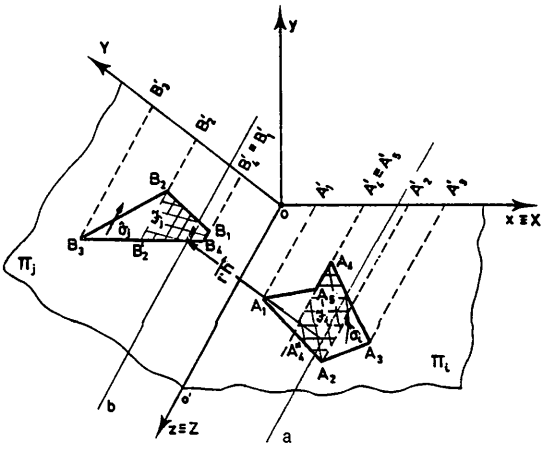

Fig. 1. Planar facets $\mathcal{F}_i$ and $\mathcal{F}_j$ are delimited by polygons $A_1, A_2, \ldots, A_5$ and $B_1, B_2, \ldots, B_4$, respectively. They lie on the half-planes Π_i and Π_j, intersecting along z. Cartesian systems $Oxyz$ and $OXYZ = OxYz$ are right-handed and the first is also orthogonal. The small bold segment of $\mathcal{F}_i$, lying on line a parallel to $\mathbf{z}$, translated by $r\hat{\mathbf{h}}$, superimposes the bold segment of $\mathcal{F}_j$, lying on line b.

length of the intersection segment, ensure the linearity of $\mathcal{P}^{(2)}_{i,j}(r)$ and allow the determination of the different subintervals as well as that of the coefficients of the relevant linear functions. Hence, the proof of (1) could already be considered accomplished.

However, for greater completeness, the contributions to $\mathcal{P}^{(2)}_{i,j}(r)$ owing to the portion of the $\mathcal{F}_i$ facet, delimited by the condition

$$\bar{x}_I \equiv x_{A'_5} < x_1 < x_{A'_2} \equiv \bar{x}_F, \tag{11}$$

and to the $\mathcal{F}_j$ portion, delimited by

$$\bar{Y}_I \equiv Y_{B'_1} < y_2 < Y_{B'_2} \equiv \bar{Y}_F \tag{12}$$

(see the hatched portions of Fig. 1), will now be explicitly worked out. The equations of (the relevant parts of) sides A_4A_3 and A_1A_2 are

$$\bar{z}_1(x_1) \equiv c_2(x_1 - \bar{x}_I) + z_{A_4} \tag{13a}$$

$$\bar{z}'_1(x_1) \equiv -c'_2(x_1 - \bar{x}_I) + z_{A''_4}. \tag{13b}$$

Here, $c_2 \equiv \cot\gamma_2$, $c'_2 \equiv \cot\gamma'_2$, while γ_2 and γ'_2 are the angles formed by $\mathbf{A_4A_3}$ and $\mathbf{A_1A_2}$ with $\hat{\mathbf{z}}$ and $-\hat{\mathbf{z}}$, respectively. Similarly, the equations of (the relevant parts of) sides B_1B_2 and B_4B_3 are

$$\bar{z}_2(Y_2) \equiv c_1(Y_2 - \bar{Y}_I) + z_{B_1} \tag{14a}$$

$$\bar{z}'_2(Y_2) \equiv -c'_1(Y_2 - \bar{Y}_I) + z_{B_4}, \tag{14b}$$

where $c_1 \equiv \cot\gamma_1$ ($c'_1 \equiv \cot\gamma'_1$), γ_1 (γ'_1) being the angle formed by $\mathbf{B_1B_2}$ ($\mathbf{B_4B_3}$) with $\hat{\mathbf{z}}$ ($-\hat{\mathbf{z}}$). The contribution to $\mathcal{P}^{(2)}_{i,j}(r)$ from the considered portions of $\mathcal{F}_i$ and $\mathcal{F}_j$ is

$$-(\hat{\mathbf{h}}\cdot\hat{\boldsymbol{\sigma}}_i)(\hat{\mathbf{h}}\cdot\hat{\boldsymbol{\sigma}}_j)\int_{\bar{Y}_I}^{\bar{Y}_F} dY_2 \int_{\bar{z}_2(Y_2)}^{\bar{z}'_2(Y_2)} dz_2 \int_{\bar{x}_I}^{\bar{x}_F} dx_1 \int_{\bar{z}_1(x_1)}^{\bar{z}'_1(x_1)} dz_1 \times \delta(\mathbf{r}_1 + r\hat{\mathbf{h}} - \mathbf{r}_2).$$

Moreover, $\mathbf{r}_1 = (x_1, 0, z_1)$, $\mathbf{r}_2 = (Y_2\cos\alpha_{ij}, Y_2\sin\alpha_{ij}, z_2)$, with $\cos\alpha_{ij} = \hat{\boldsymbol{\sigma}}_i \cdot \hat{\boldsymbol{\sigma}}_j$. The integral is evaluated by the procedure expounded in Appendix A of I. Its final expression is

$$-\{[(\hat{\mathbf{h}}\cdot\hat{\boldsymbol{\sigma}}_i)(\hat{\mathbf{h}}\cdot\hat{\boldsymbol{\sigma}}_j)]/\sin\alpha_{ij}\}\max[L_{\max} - L_{\min}, 0], \tag{15}$$

where

$$L_{\max} \equiv \min[\bar{z}'_1(r\hat{h}_y\cot\alpha_{ij} - rm_x) + r\hat{h}_z; \bar{z}'_2(r\hat{h}_y/\sin\alpha_{ij})] \tag{16a}$$

$$L_{\min} \equiv \max[\bar{z}_1(r\hat{h}_y\cot\alpha_{ij} - r\hat{h}_x) + r\hat{h}_z; \bar{z}_2(r\hat{h}_y/\sin\alpha_{ij})] \tag{16b}$$

with the following constraints on r:

$$r \le \min\left[\frac{\bar{Y}_F\sin\alpha_{ij}}{\hat{h}_y}, \frac{\bar{x}_F\sin\alpha_{ij}}{\hat{h}_y\cos\alpha_{ij} - \hat{h}_x\sin\alpha_{ij}}\right] \equiv R_1 \tag{17a}$$

$$r \ge \max\left[\frac{\bar{Y}_I\sin\alpha_{ij}}{\hat{h}_y}, \frac{\bar{x}_I\sin\alpha_{ij}}{\hat{h}_y\cos\alpha_{ij} - \hat{h}_x\sin\alpha_{ij}}\right] \equiv R_2 \tag{17b}$$

and

$$\hat{\mathbf{h}} \equiv (\hat{h}_x, \hat{h}_y, \hat{h}_z).$$

It is emphasized that (15) is a *linear* r function, owing to definitions (16*a*), (16*b*), (13) and (14). Clearly, whenever constraints (17*a*) and (17*b*) were not simultaneously obeyed, the considered portions of the pair of facets $\mathcal{F}_i$ and $\mathcal{F}_j$ would yield a null contribution to $\mathcal{P}^{(2)}_{i,j}(r)$. In contrast, interval $[R_1, R_2]$ splits into two subintervals $[R_1, R']$ and $[R', R_2]$, depending on the value assumed by (15). Only the subinterval where inequality $L_{\max} > L_{\min}$ takes place must be considered, otherwise the contribution to $\mathcal{P}^{(2)}_{i,j}(r)$ is null. In general, this subinterval splits into smaller subintervals determined by the values of $L_{\max}$ and $L_{\min}$ resulting from definitions (16*a*) and (16*b*). In this way, the r subintervals and the associated expressions for the contributions to $\mathcal{P}^{(2)}_{i,j}(r)$ arising from the considered portions of the pair of facets $\mathcal{F}_i$ and $\mathcal{F}_j$ are obtained. In any case, these contributions are *linear* r functions. Of course, in order to fully determine $\mathcal{P}^{(2)}_{i,j}(r)$, the contributions arising from all the other possible pairs of the remaining portions of $\mathcal{F}_i$ and $\mathcal{F}_j$ must be taken into account. Their evaluation can be similarly carried through. In this way, the *linear* expressions for $\mathcal{P}^{(2)}_{i,j}(r)$ and the corresponding r intervals [whose extrema are the $D_{ij,k}$'s used below (10*a*)] turn out to be determined and (1) is proven.

4. Scherrer constant expressions

For powder samples, consisting of *equal* crystallites (*equal* means that the crystallites have the same size and the same shape), the assumption that cross-interference contributions are negligible allows us to write

$$V_F^{-1}\int_{R^3} dv_1\, \rho_F(\mathbf{r}_1 + r\hat{\mathbf{h}})\rho_F(\mathbf{r}_1) \simeq V^{-1}\int_V dv_1\, \rho_c(\mathbf{r}_1 + r\hat{\mathbf{h}})\rho_c(\mathbf{r}_1), \tag{18}$$

where $\rho_c(\mathbf{r})$ is now the characteristic function of a single crystallite [*i.e.* $\rho_c(\mathbf{r}) = 1$ only when the tip of $\mathbf{r}$ falls inside the considered crystallite] and V is the latter's volume (Ciccariello, 1990, §§II and III). The

peak profile, observed around reflection $\mathbf{h}$, is the Fourier transform of the right-hand side (r.h.s.) of (18).

The relations existing between crystallites' shapes/sizes and Scherrer constants as well as the way of determining the latter from observed peak profiles have been thoroughly reviewed by Langford & Wilson (1978). Their definitions will now be recalled. The apparent crystallite sizes ε_K and ε_T, along reflection $\mathbf{h}$, are related to the values of the first and second derivative of the corresponding OF at the origin by [see equations (5) and (9)* of Langford & Wilson (1978)]

$$\varepsilon_K = -V/V'_{\hat{\mathbf{h}}}(0^+) \tag{19}$$

$$\varepsilon_T^2 = V/V''_{\hat{\mathbf{h}}}(0^+). \tag{20}$$

The Scherrer constants $\mathcal{K}_K$ and $\mathcal{K}_T$ are dimensionless quantities related to the reciprocals of the former quantities by

$$\mathcal{K}_K = \langle L\rangle\varepsilon_K^{-1} = \langle L\rangle^{-2}V'_{\hat{\mathbf{h}}}(0^+) \tag{21a}$$

$$\mathcal{K}_T^2 = \langle L\rangle^2\varepsilon_T^{-2} = \langle L\rangle^{-1}V''_{\hat{\mathbf{h}}}(0^+) \equiv \mathcal{L}, \tag{21b}$$

where $\langle L\rangle$ represents an average linear size of the particle obtained by the latter's volume through

$$\langle L\rangle \equiv V^{1/3}. \tag{21c}$$

A further quantity $\mathcal{M}$, the *rotundity* parameter (Wilson, 1971), first introduced by Mitra (1964), is defined as

$$\mathcal{M} = -V'''_{\hat{\mathbf{h}}}(0^+). \tag{22}$$

$\mathcal{M}$, being a dimensionless quantity, is independent of the particle size and only depends on the shape. It is recalled that $\langle L\rangle^2\mathcal{K}_K = \mathcal{S}$, where $\mathcal{S}$ is the area of the projection of the crystallite surface onto a plane orthogonal to $\mathbf{h}$, the observed reflection (Wilson, 1962*a*). Moreover, $\mathcal{K}_T$ differs from zero only when edges are present on the crystallite surface and increases as the dihedral angles become smaller, as was first pointed out by Wilson (1962*b*) in introducing this quantity. [Actually, Wilson called *taper* the quantity $\mathcal{L}$ $(= \mathcal{K}_T^2)$.] So far, it appears that $\mathcal{K}_T$ and $\mathcal{M}$ are explicitly known only for the following shapes: sphere and hemisphere, rectangular parallelepipeds and right prisms, tetrahedra, octahedra and right circular cylinders. For the hemispherical and cylindrical shapes, the $\mathcal{K}_T$ and $\mathcal{M}$ expressions were worked out by Wilson (1969) and by Langford & Louër (1982), while for the polyhedra the expressions were obtained by Wilson (1969, 1971) and by Edwards & Toman (1971) starting from the corresponding OF expressions worked out by Stokes & Wilson (1942). Numerical tabulations of $\mathcal{K}_K$, $\mathcal{K}_T$ and $\mathcal{M}$ are also available for most of these shapes (Wilson, 1971; Edwards & Toman, 1971; Langford & Wilson, 1978; Langford & Louër, 1982).

From (10*a*) and (15) of §3, it is possible to obtain the explicit expressions for $\mathcal{K}_T$ and $\mathcal{M}$ whatever the crystallite shape, provided the latter's surface consists of planar facets. To this aim, it is necessary to evaluate $V''_{\hat{\mathbf{h}}}(0^+)$ and $V'''_{\hat{\mathbf{h}}}(0^+)$. Since $r = 0^+$, the sum on the r.h.s. of (10*a*) will now involve the only pairs of facets that have one edge or one vertex in common. [See the paragraph below (10*b*).] Therefore, the expression for $\mathcal{P}^{(2)}_{i,j}(r)$, when $\mathcal{F}_i$ and $\mathcal{F}_j$ share a point or a segment, must first be obtained at $r \simeq 0$. The expression can easily be obtained by (15)–(17). In fact, the case of two facets having an edge in common can easily be obtained from Fig. 1. To this aim, it must be assumed that facet $\mathcal{F}_i$ does not contain the portion on the left of segment A''_4A_4 and that this edge of $\mathcal{F}_i$ lies on axis z and coincides with edge B_4B_1 of facet $\mathcal{F}_j$. The resulting configuration requires that in (13) and (14)

$$\bar{z}_{A_4} = \bar{z}_{B_1}, \tag{23a}$$

$$\bar{z}_{A''_4} = \bar{z}_{B_4}, \tag{23b}$$

$$x_{A_4} = x_{A''_4} = \bar{x}_I = 0, \tag{23c}$$

$$Y_{B_4} = Y_{B_1} = \bar{Y}_I = 0, \tag{23d}$$

while the length of the edge in common is

$$L_{ij} = \bar{z}_{A''_4} - \bar{z}_{A_4}. \tag{23e}$$

It is noted that the case of two facets having only a vertex in common amounts to setting $L_{ij} = 0$ in (23*e*), *i.e.* to have $\bar{z}_{A_4} = \bar{z}_{B_1} = \bar{z}_{A''_4} = \bar{z}_{B_4}$. Consider first the case $L_{ij} > 0$. From (15) and (16) at very small r's,

$$\mathcal{P}^{(2)}_{i,j}(r) = -\frac{(\hat{\boldsymbol{\sigma}}_i\cdot\hat{\mathbf{h}})(\hat{\boldsymbol{\sigma}}_j\cdot\hat{\mathbf{h}})}{[1-(\hat{\boldsymbol{\sigma}}_i\cdot\hat{\boldsymbol{\sigma}}_j)^2]^{1/2}} \times \max[L_{ij} - r(\mathcal{W}_{ij} + \mathcal{W}'_{ij}), 0], \tag{24}$$

with*

$$\mathcal{W}_{ij} \equiv \max[c_2(\hat{h}_y\cot\alpha_{ij} - \hat{h}_x), c_1\hat{h}_y/\sin\alpha_{ij} - \hat{h}_z] \tag{25a}$$

$$\mathcal{W}'_{ij} \equiv \max[c'_2(\hat{h}_y\cot\alpha_{ij} - \hat{h}_x), c'_1\hat{h}_y/\sin\alpha_{ij} + \hat{h}_z]. \tag{25b}$$

For (24) to be written in a covariant way, it is first observed that the unit vectors of the considered Cartesian

* The l.h.s. of this equation lacks the exponent 2. The exponent is required for consistency with equations (19) and (27) of Langford & Wilson (1978).

* Equations (24) and (25) coincide with equations (I-2.8), (I-2.9) and (I-2.20) but the following misprints must be corrected: c_1 and c_2 must be interchanged in equation (I-2.9*a*); the 1 on the r.h.s. of equation (I-2.1) must be cancelled out.

axes can be expressed in terms of $\hat{\sigma}_i$ and $\hat{\sigma}_j$ by the following relations:

$$\hat{\mathbf{y}} = \hat{\sigma}_i, \quad \hat{\mathbf{z}} = \frac{\hat{\sigma}_j \times \hat{\sigma}_i}{\|\hat{\sigma}_i \times \hat{\sigma}_j\|}, \quad \hat{\mathbf{x}} = \frac{\hat{\sigma}_j - \hat{\sigma}_i(\hat{\sigma}_i \cdot \hat{\sigma}_j)}{\|\hat{\sigma}_i \times \hat{\sigma}_j\|}. \tag{26}$$

Then, let $\hat{\mathbf{e}}_{i,1}$ ($\hat{\mathbf{e}}_{i,2}$) and $\hat{\mathbf{e}}_{j,1}$ ($\hat{\mathbf{e}}_{j,2}$) denote the unit vectors of the edges coming out from $B_1 = A_4$ ($B_4 = A_4''$) and lying, respectively, on $\mathcal{F}_i$ and $\mathcal{F}_j$. It is easy to show that

$$c_2 = \frac{\hat{\mathbf{e}}_{i,1} \cdot (\hat{\sigma}_j \times \hat{\sigma}_i)}{\{\|\hat{\sigma}_i \times \hat{\sigma}_j\|^2 - [\hat{\mathbf{e}}_{i,1} \cdot (\hat{\sigma}_j \times \hat{\sigma}_i)]^2\}^{1/2}} \tag{27a}$$

$$c_2' = -\frac{\hat{\mathbf{e}}_{i,2} \cdot (\hat{\sigma}_j \times \hat{\sigma}_i)}{\{\|\hat{\sigma}_i \times \hat{\sigma}_j\|^2 - [\hat{\mathbf{e}}_{i,2} \cdot (\hat{\sigma}_j \times \hat{\sigma}_i)]^2\}^{1/2}}. \tag{27b}$$

The expressions for c_1 and c_1' are obtained by substituting $\hat{\mathbf{e}}_{i,1}$ with $\hat{\mathbf{e}}_{j,1}$ in (27*a*) and $\hat{\mathbf{e}}_{i,2}$ with $\hat{\mathbf{e}}_{j,2}$ in (27*b*), respectively. Hence, (25*a*) and (25*b*) become

$$\mathcal{W}_{ij} = (1/\|\hat{\sigma}_i \times \hat{\sigma}_j\|) \times \max\left(\frac{-(\hat{\mathbf{h}} \cdot \hat{\sigma}_j)[\hat{\mathbf{e}}_{i,1} \cdot (\hat{\sigma}_j \times \hat{\sigma}_i)]}{\{\|\hat{\sigma}_i \times \hat{\sigma}_j\|^2 - [\hat{\mathbf{e}}_{i,1} \cdot (\hat{\sigma}_j \times \hat{\sigma}_i)]^2\}^{1/2}}, \frac{(\hat{\mathbf{h}} \cdot \hat{\sigma}_i)[\hat{\mathbf{e}}_{j,1} \cdot (\hat{\sigma}_j \times \hat{\sigma}_i)]}{\{\|\hat{\sigma}_i \times \hat{\sigma}_j\|^2 - [\hat{\mathbf{e}}_{j,1} \cdot (\hat{\sigma}_j \times \hat{\sigma}_i)]^2\}^{1/2}} - \hat{\mathbf{h}} \cdot (\hat{\sigma}_j \times \hat{\sigma}_i) \right), \tag{28a}$$

$$\mathcal{W}_{ij}' = (1/\|\hat{\sigma}_i \times \hat{\sigma}_j\|) \times \max\left(\frac{(\hat{\mathbf{h}} \cdot \hat{\sigma}_j)[\hat{\mathbf{e}}_{i,2} \cdot (\hat{\sigma}_j \times \hat{\sigma}_i)]}{\{\|\hat{\sigma}_i \times \hat{\sigma}_j\|^2 - [\hat{\mathbf{e}}_{i,2} \cdot (\hat{\sigma}_j \times \hat{\sigma}_i)]^2\}^{1/2}}, \hat{\mathbf{h}} \cdot (\hat{\sigma}_j \times \hat{\sigma}_i) - \frac{(\hat{\mathbf{h}} \cdot \hat{\sigma}_i)[\hat{\mathbf{e}}_{j,2} \cdot (\hat{\sigma}_j \times \hat{\sigma}_i)]}{\{\|\hat{\sigma}_i \times \hat{\sigma}_j\|^2 - [\hat{\mathbf{e}}_{j,2} \cdot (\hat{\sigma}_j \times \hat{\sigma}_i)]^2\}^{1/2}} \right). \tag{28b}$$

Finally, constraints (17*a*) and (17*b*) simplify into

$$\hat{\mathbf{h}} \cdot \hat{\sigma}_i > 0 \quad \text{and} \quad \hat{\mathbf{h}} \cdot \hat{\sigma}_j < 0. \tag{28c}$$

The expressions for $V_{\hat{\mathbf{h}}}''(0^+)$ and $V_{\hat{\mathbf{h}}}'''(0^+)$ are now obtained. Equation (24) shows that $\mathcal{P}_{i,j}^{(2)}(0^+)$ is proportional to L_{ij}, the length of the edge shared by the relevant facets. Hence, by (20) and (21*b*),

$$\mathcal{K}_T^2 = -(2/\langle L \rangle) \sum_{i<j}{}' [L_{ij}(\hat{\mathbf{h}} \cdot \hat{\sigma}_i)(\hat{\mathbf{h}} \cdot \hat{\sigma}_j)\Theta(\mathbf{h} \cdot \hat{\sigma}_i) \times \Theta(-\mathbf{h} \cdot \hat{\sigma}_j)]/\|\hat{\sigma}_i \times \hat{\sigma}_j\|. \tag{29}$$

Here, Θ denotes the step function, while the prime on the summation is a reminder that only pairs of facets having one edge in common are involved in (29). It should be noted that the contribution to $\mathcal{K}_T$ resulting from an edge, *e.g.* the one intersection of facets $\mathcal{F}_i$ and $\mathcal{F}_j$, becomes very large when the dihedral angle between facets $\mathcal{F}_i$ and $\mathcal{F}_j$ is close to 0 because the denominator tends to zero and the constraints relevant to the two step functions can be simultaneously fulfilled. (On the contrary, when the dihedral angle approaches π, one of the constraints is violated and the contribution becomes null.)

In order to obtain the rotundity expression, it is first remarked that when the common edge has a finite length, function max, present on the r.h.s. of (24), simply reduces to $L_{ij} - r(\mathcal{W}_{ij} + \mathcal{W}_{ij}')$, provided r is sufficiently small. In this case, the derivative of $\mathcal{P}_{i,j}^{(2)}(r)$ is the sum of contributions $-\mathcal{W}_{ij}$ and $-\mathcal{W}_{ij}'$. Since each of these involves only the angles relevant to one of the ends of the common edge, $-\mathcal{W}_{ij}$ can be assigned to one end and $-\mathcal{W}_{ij}'$ to the opposite end. In this way, the contributions to $V_{\hat{\mathbf{h}}}'''(0^+)$ can be regrouped according to the vertices of the crystallite. In fact, for each vertex $\mathcal{V}$, one must consider the different pairs of facets meeting only at $\mathcal{V}$ and the pairs of facets that meet along the edges coming out from $\mathcal{V}$. The contributions to $V_{\hat{\mathbf{h}}}''(0^+)$, originating from the latter pairs, are proportional to the relevant $\mathcal{W}_{ij}$'s. In order to obtain those relevant to the first class of facet pairs, in (24) L_{ij} is assumed to be zero. Hence, the contribution of $\mathcal{P}_{i,j}^{(3)}(r)$ will be $-(\mathcal{W}_{ij} + \mathcal{W}_{ij}')$, provided this quantity is greater than zero. Therefore, with

$$\mathcal{V}_{ij}^{(3)} \equiv \mathcal{W}_{ij} \tag{30}$$

and

$$\mathcal{V}_{ij}^{(4)} \equiv (\mathcal{W}_{ij} + \mathcal{W}_{ij}')\Theta(-\mathcal{W}_{ij} - \mathcal{W}_{ij}'), \tag{31}$$

$\mathcal{M}$ will be given by

$$\mathcal{M} = 2 \sum_{\mathcal{V}} \sum_{i<j}{}'' \{[(\hat{\mathbf{h}} \cdot \hat{\sigma}_i)(\hat{\mathbf{h}} \cdot \hat{\sigma}_j)\Theta(\mathbf{h} \cdot \hat{\sigma}_i)\Theta(-\mathbf{h} \cdot \hat{\sigma}_j)] \times (\|\hat{\sigma}_i \times \hat{\sigma}_j\|)^{-1}\}[\mathcal{V}_{ij}^{(3)} + \mathcal{V}_{ij}^{(4)}], \tag{32}$$

where the double prime on the summation is a reminder that only the facet pairs that meet at the considered vertex $\mathcal{V}$ must be considered.

From (29) and (32), it is easy to recover the results already obtained by Wilson and co-workers. For further illustration, the numerical values of the Scherrer constants and of the rotundity have been calculated by (29) and (32) for the dodecahedron, the icosahedron and a triclinic parallelepiped. The calculations, rather straightforward by a computer, require only some care in labeling all the vectors involved in (28). The results* for a triclinic parallelepiped are reported in Table 1 while

* The related computer program will be made available on request.

Table 1. *Triclinic parallelepiped*

The triclinic cell is characterized by the angles: $\arccos(\mathbf{a}\cdot\mathbf{b}) = \pi/5$, $\arccos(\mathbf{a}\cdot\mathbf{c}) = \pi/4$ and $\arccos(\mathbf{b}\cdot\mathbf{c}) = \pi/3$, while the edges of the parallelepipeds are respectively equal to Na, $2Nb$ and $3Nc$, N being an arbitrary positive integer. The first column reports the $\mathbf{h}$ components in units of the reciprocal space. The corresponding values of $\mathcal{K}_K$, $\mathcal{K}_T$ and $\mathcal{M}$ are reported in the second, third and fourth columns, respectively.

hkl	$\mathcal{K}_K$	$\mathcal{K}_T$	$\mathcal{M}$	hkl	$\mathcal{K}_K$	$\mathcal{K}_T$	$\mathcal{M}$	hkl	$\mathcal{K}_K$	$\mathcal{K}_T$	$\mathcal{M}$
(100)	4.1051	2.7938	4.9189	(3$\bar{2}$1)	3.9605	2.7138	3.8238	(430)	2.9694	1.8293	3.7918
(110)	2.2282	1.4073	2.2848	(3$\bar{2}\bar{1}$)	4.1570	2.8896	5.5769	(4$\bar{3}$0)	4.0924	2.8311	4.7632
(1$\bar{1}$0)	4.0541	2.8115	4.6987	(322)	2.2568	1.1728	0.5807	(431)	2.7816	1.6317	2.5289
(111)	0.7298	0.5412	0.2575	(32$\bar{2}$)	3.1843	2.0971	5.8989	(43$\bar{1}$)	3.0247	1.9151	4.7666
(11$\bar{1}$)	2.4725	1.5429	4.6382	(3$\bar{2}$2)	3.6988	2.5018	2.7016	(4$\bar{3}$1)	3.9938	2.7466	4.0876
(1$\bar{1}$1)	3.3675	2.2568	1.8404	(3$\bar{2}\bar{2}$)	4.1494	2.8960	6.2577	(4$\bar{3}\bar{1}$)	4.1431	2.8789	5.3036
(1$\bar{1}\bar{1}$)	4.1318	2.9000	6.4681	(331)	1.8563	1.2231	1.1254	(432)	2.3286	1.2218	1.0831
(210)	3.6327	2.3780	4.6336	(33$\bar{1}$)	2.3558	1.4416	3.4773	(43$\bar{2}$)	3.0247	1.9489	5.3265
(2$\bar{1}$0)	4.1245	2.8434	4.7869	(3$\bar{3}$1)	3.9112	2.6921	3.8360	(4$\bar{3}$2)	3.8366	2.6179	3.2906
(211)	3.2808	2.0364	2.0003	(3$\bar{3}\bar{1}$)	4.1268	2.8771	5.3564	(4$\bar{3}\bar{2}$)	4.1573	2.8986	5.8736
(21$\bar{1}$)	3.5280	2.3579	6.2176	(332)	1.0657	0.7107	0.2072	(433)	1.5864	0.6285	0.1509
(2$\bar{1}$1)	3.8614	2.6208	3.1826	(33$\bar{2}$)	2.4014	1.4497	4.1977	(43$\bar{3}$)	3.0038	1.9589	5.6356
(2$\bar{1}\bar{1}$)	4.1551	2.8888	6.0871	(3$\bar{3}$2)	3.6835	2.5083	2.8361	(4$\bar{3}$3)	3.6146	2.4399	2.4687
(221)	1.5140	1.0185	0.5920	(3$\bar{3}\bar{2}$)	4.1471	2.9025	5.9677	(4$\bar{3}\bar{3}$)	4.1454	2.8980	6.3234
(22$\bar{1}$)	2.3788	1.4377	3.8841	(410)	3.9706	2.6665	4.7803	(441)	1.9843	1.2925	1.4190
(2$\bar{2}$1)	3.8085	2.6087	3.3460	(4$\bar{1}$0)	4.1377	2.8382	4.8749	(44$\bar{1}$)	2.3367	1.4399	3.2290
(2$\bar{2}\bar{1}$)	4.1423	2.8940	5.6562	(411)	3.9218	2.6025	3.4616	(4$\bar{4}$1)	3.9544	2.7277	4.0684
(310)	3.8869	2.5932	4.6661	(41$\bar{1}$)	3.9292	2.6598	5.8314	(4$\bar{4}\bar{1}$)	4.1142	2.8650	5.2123
(3$\bar{1}$0)	4.1366	2.8429	4.8401	(4$\bar{1}$1)	4.0545	2.7603	3.9561	(442)	1.5140	1.0185	0.5920
(311)	3.7871	2.4772	3.1040	(4$\bar{1}\bar{1}$)	4.1513	2.8628	5.6774	(44$\bar{2}$)	2.3788	1.4377	3.8841
(31$\bar{1}$)	3.8169	2.5754	6.0948	(420)	3.6327	2.3780	4.6336	(4$\bar{4}$2)	3.8085	2.6087	3.3460
(3$\bar{1}$1)	4.0010	2.7220	3.7090	(4$\bar{2}$0)	4.1245	2.8434	4.7869	(4$\bar{4}\bar{2}$)	4.1423	2.8940	5.6562
(3$\bar{1}\bar{1}$)	4.1552	2.8744	5.8413	(421)	3.5668	2.2903	3.2968	(443)	0.9619	0.7175	0.3089
(320)	3.2316	2.0461	4.2007	(42$\bar{1}$)	3.5979	2.3844	5.6218	(44$\bar{3}$)	2.4236	1.4778	4.3312
(3$\bar{2}$0)	4.1042	2.8363	4.7774	(4$\bar{2}$1)	4.0306	2.7606	4.0656	(4$\bar{4}$3)	3.6126	2.4517	2.5930
(321)	3.0074	1.8115	2.3791	(4$\bar{2}\bar{1}$)	4.1602	2.8819	5.5014	(4$\bar{4}\bar{3}$)	4.1460	2.9040	6.1077
(32$\bar{1}$)	3.2375	2.1012	5.3757								

those relevant to dodecahedra and icosahedra are shown in Figs. 2 and 3.

5. Functional expression of peak profiles

Our last remark concerns the functional form of the peak profiles scattered by a powder sample of *equal* crystallites with planar facets. The basic relation between the OF and the peak profile $I_{\mathbf{h}}(s)$ around reflection $\mathbf{h}$ is (Guinier, 1963; Wilson, 1962*a*)

$$i_{\mathbf{h}}(s) \equiv I_{\mathbf{h}}(s)/\mathcal{C} = V^{-1}\int_{-\infty}^{\infty} \exp(iqt)V_{\hat{\mathbf{h}}}(t)\,\mathrm{d}t \quad (q \equiv 2\pi s), \tag{33}$$

$\mathcal{C}$ being a suitable normalization constant. The parity property (4*b*) yields

$$i_{\mathbf{h}}(s) = (2/V)\int_0^{\infty} V_{\hat{\mathbf{h}}}(t)\cos(qt)\,\mathrm{d}t, \tag{34}$$

and from the condition $V_{\hat{\mathbf{h}}}(0) = V$ it follows that

$$2\pi\int_{-\infty}^{\infty} i_{\mathbf{h}}(s)\,\mathrm{d}s = 1. \tag{35}$$

For this reason, $i_{\mathbf{h}}(s)$ is referred to as the *normalized* peak profile.

The most general expression of a peak profile is immediately obtained by substituting (1) into (33). Straightforward calculations yield

$$\begin{aligned} i_{\mathbf{h}}(s)/2 = {} & \mathcal{S}/Vq^2 - \mathcal{M}/Vq^4 \\ & + \sum_{i=1}^{N}\{[\mathcal{I}_{1,i}\cos(qD_i)]/q^2 \\ & + [\mathcal{I}_{2,i}\sin(qD_i)]/q^3 \\ & + [\mathcal{I}_{3,i}\cos(qD_i)]/q^4\}/V, \end{aligned} \tag{36}$$

where

$$\mathcal{I}_{1,i} \equiv \Gamma_{1,i-1} - \Gamma_{1,i} + 2\Gamma_{2,i-1}(D_i - D_{i-1}) + 3\Gamma_{3,i-1}(D_i - D_{i-1})^2, \tag{37a}$$

$$\mathcal{I}_{2,i} \equiv -2[\Gamma_{2,i-1} - \Gamma_{2,i} + 3\Gamma_{3,i-1}(D_i - D_{i-1})], \tag{37b}$$

$$\mathcal{I}_{3,i} \equiv -6(\Gamma_{3,i-1} - \Gamma_{3,i}), \tag{37c}$$

with

$$\Gamma_{\ell,N} \equiv 0, \quad \ell = 1, 2, 3.$$

Here, $\mathcal{S} = \mathcal{K}_K\langle L\rangle^2$ is the area of the projection of the particle onto a plane orthogonal to $\mathbf{h}$. In obtaining (36), conditions (5) resulting from the continuity of $V_{\hat{\mathbf{h}}}(r)$ have been taken into account. For this reason, no $\Gamma_{0,i}$

is present in (36). It is stressed that (36) is an exact result for locally planar interfaces. Therefore, it makes sense throughout the physical range $[0, \infty]$ of q and the singular contributions exactly cancel as $q \to 0$. It is recalled that equation (10.71) of Wilson (1970) contains *in nuce* result (36). Indeed, the planarity of facets ensures that his $V^{IV}_{\hat{\mathbf{h}}}(t)$ (*i.e.* the fourth derivative of the OF) is identically null so that the integral contribution in (10.71) vanishes. The evaluation of the remaining terms requires that first-order discontinuities of $V'_{\hat{\mathbf{h}}}(t)$, $V''_{\hat{\mathbf{h}}}(t)$ and $V'''_{\hat{\mathbf{h}}}(t)$ are properly taken into account. Ultimately, in fact, these are responsible for the contributions present on the r.h.s. of (36). It is also remarked that altogether the three peak profiles* reported by Grebille & Bérar (1985) contain the terms present in (36). The last remark concerns the fact that it can reasonably be expected that the oscillatory contributions, present in (36), average to zero at large q. In this way, only the first two terms on the r.h.s. of (36) need be taken into account when the *tails* [see §VI of Ciccariello (1990)] of peak profiles are analyzed. A simple best fit would determine both the surface ($\propto \mathcal{K}_K$) and the rotundity ($\mathcal{M}$) of the crystallite, while $\mathcal{K}_T$ can be determined either by the sum rule, first noted by Porod (1967) in the small-angle scattering realm and generalized by Ciccariello (1990) to the case of wide-angle scattering, or by the procedure described by Wilson (1971).

Finally, the more realistic case of polydisperse samples of crystallites with equal shapes and different sizes L can be treated in the usual approximation of considering only self-interference effects of particles with the same size. Let $p(L)$ denote the normalized number density of the particles with sizes ranging in the infinitesimal interval $[L, L + \mathrm{d}L]$. Then, it appears more likely that the oscillatory contributions on the r.h.s. of (36) average to zero, while the q^{-2} and q^{-4} coefficients on the r.h.s. of (36), respectively, become

$$(\mathcal{S}_{\hat{\mathbf{h}}}/V)_1 \int_0^\infty L^{-1} p(L)\, \mathrm{d}L$$

and

$$\mathcal{M}_{\hat{\mathbf{h}}} \int_0^\infty L^{-3} p(L)\, \mathrm{d}L,$$

* These have to be multiplied by 2 if A gives the area of the right section of the prism.

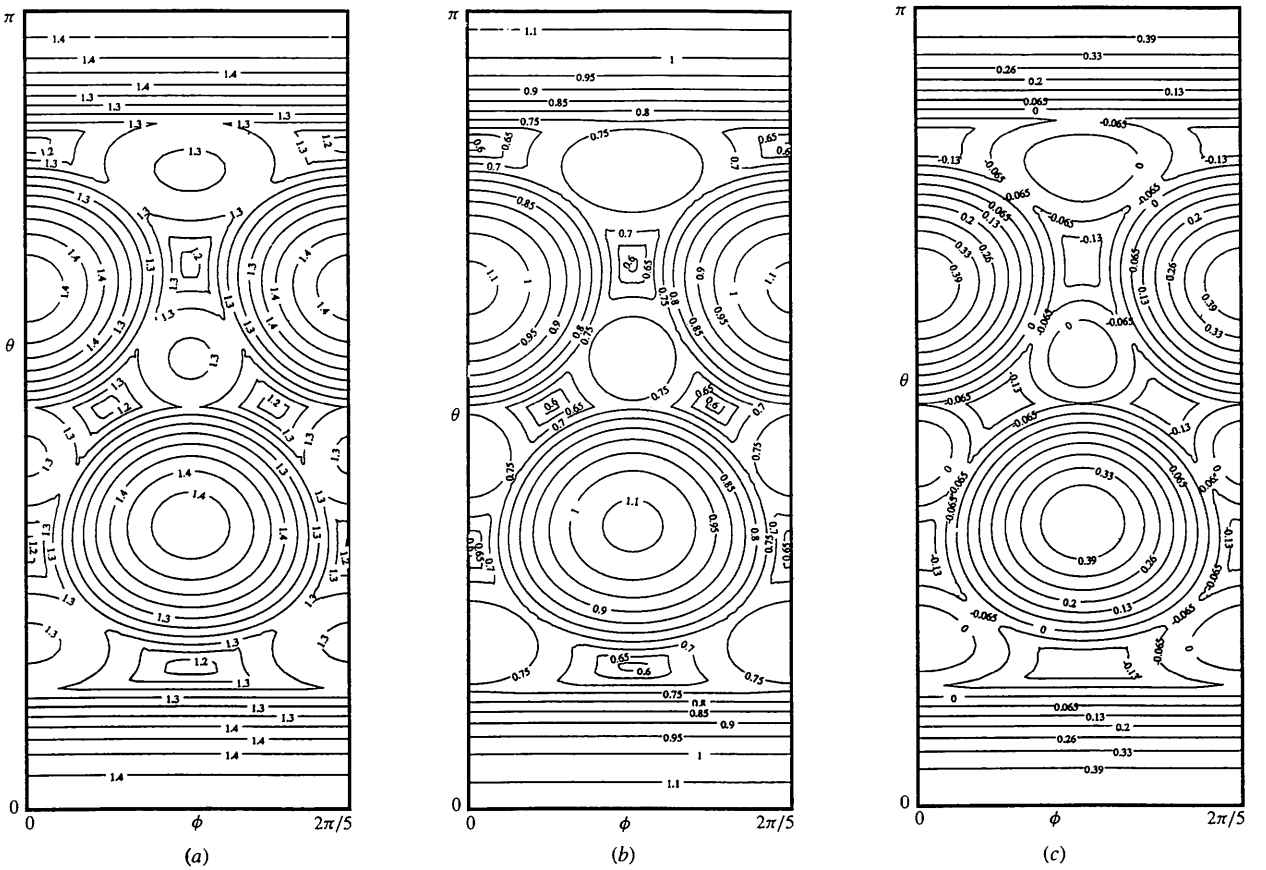

Fig. 2. (*a*), (*b*) and (*c*) respectively show the relief lines of $\mathcal{K}_K$, $\mathcal{K}_T$ and $\mathcal{M}$ for a dodecahedron in terms of the polar (θ) and longitudinal (ϕ) angles of $\hat{\mathbf{h}}$ with respect to a Cartesian frame having its origin at the center of the dodecahedron, the z axis orthogonal to one facet and the $(xz, x > 0)$ half-plane going through a vertex of the considered facet.

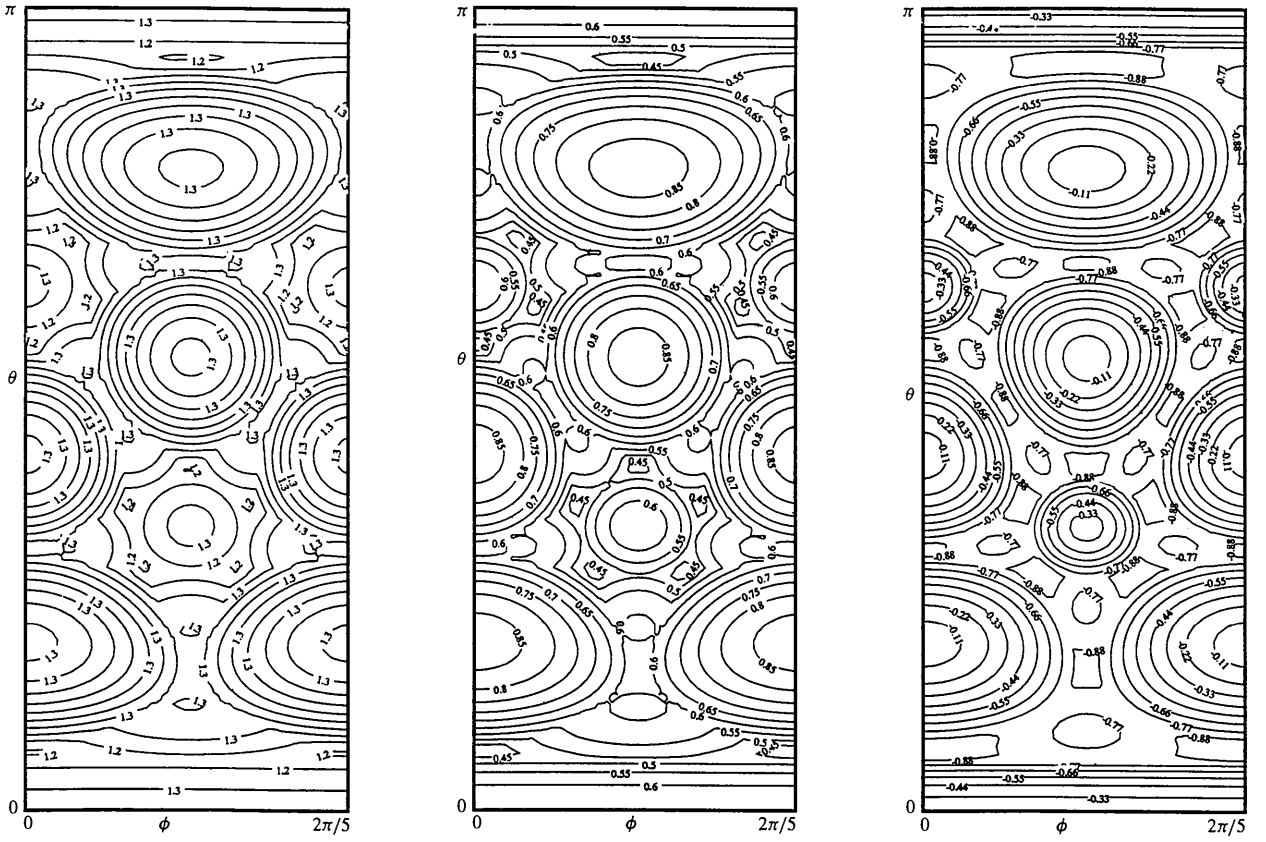

Fig. 3. (*a*), (*b*) and (*c*) respectively show the relief lines of $\mathcal{K}_K$, $\mathcal{K}_T$ and $\mathcal{M}$ for an icosahedron in terms of the polar (θ) and longitudinal (ϕ) angles of $\hat{\mathbf{h}}$ with respect to a Cartesian frame having its origin at the center of the icosahedron, the z axis going through a vertex and the $(xz, x > 0)$ half-plane bisecting one side of the (upper) regular pentagon parallel to the xy plane.

where subscript $\hat{\mathbf{h}}$ makes the dependence of the quantity on $\hat{\mathbf{h}}$ more evident and subscript 1 denotes that the ratio refers to a crystallite of size $L = 1$. Since the integrals do not depend on the considered reflection while $(\mathcal{S}_{\hat{\mathbf{h}}}/V)_1$ and $\mathcal{M}_{\hat{\mathbf{h}}}$ do, the analysis of different peak profiles allows one to determine the ratios $(\mathcal{S}_{\hat{\mathbf{h}}}/V)_1/(\mathcal{S}_{\hat{\mathbf{h}}'}/V)_1$ and $\mathcal{M}_{\hat{\mathbf{h}}}/\mathcal{M}_{\hat{\mathbf{h}}'}$ independently of the particle distributions.

Financial support to SC from the MURST through 40% and 60% funds are gratefully acknowledged.

References

Ciccariello, S. (1985). *Acta Cryst.* A**41**, 560–568.
Ciccariello, S. (1990). *Acta Cryst.* A**46**, 175–186.
Ciccariello, S. & Sobry, R. (1995). *Acta Cryst.* A**51**, 60–69.
Debye, P., Anderson, H. R. & Brumberger, H. (1957). *J. Appl. Phys.* **28**, 679–683.
Edwards, H. J. & Toman, K. (1971). *J. Appl. Cryst.* **4**, 319–321.
Grebille D. & Bérar J.-F. (1985). *J. Appl. Cryst.* **18**, 301–307
Guinier, A. (1963). *X-ray Diffraction.* San Francisco: Freeman.
Langford, J. I. & Louër D. (1982). *J. Appl. Cryst.* **15**, 20–26.
Langford, J. I. & Wilson, A. J. C. (1978). *J. Appl. Cryst.* **11**, 102–113.
Mitra, B. G. (1964). *Br. J. Appl. Phys.* **15**, 917–921.
Porod, G. (1967). *Small Angle X-ray Scattering. Proceedings of the Syracuse Conference*, edited by H. Brumberger, pp. 1–15. New York: Gordon and Breach.
Stokes, A. R. & Wilson, A. J. C. (1942). *Proc. Cambridge Philos. Soc.* **38**, 313–322.
Wilson, A. J. C. (1962*a*). *X-ray Optics*, 2nd ed. London: Methuen.
Wilson, A. J. C. (1962*b*). *Proc. Phys. Soc. London*, **80**, 286–294.
Wilson, A. J. C. (1969). *J. Appl. Cryst.* **2**, 181–183.
Wilson, A. J. C. (1970). *Elements of X-ray Crystallography*, ch. 10. Reading, MA: Addison-Wesley.
Wilson, A. J. C. (1971). *J. Appl. Cryst.* **4**, 440–443.